The Integrated Precipitation and Hydrology Experiment - Hydrologic Applications for the Southeast US (IPHEx-H4SE)

Part III: High-Resolution Ensemble Rainfall Products

http://iphex.pratt.duke.edu

Miguel Nogueira and Ana P. Barros

EPL-2013-IPHEX-H4SE-3

January 14, 2014 – V1.0

Acknowledgment: This work was supported by NASA's Precipitation Measurement Missions Program and GPM Ground Validation.

Citation: Nogueira, M. and Barros, A.P., 2013: The Integrated Precipitation and Hydrology Experiment. Part III: High-Resolution Ensemble Rainfall Products

Report EPL-2013-IPHEX-H4SE-3, EPL/Duke University (Pub.), 38pp. DoI: Duke University Libraries (request pending)

Data Availability: http://iphex.pratt.duke.edu

Disclaimer: This purpose of this report is to provide background information on the generation of IPHEX-H4SE data sets. Results are presented for the first five years. The same methods were used for subsequent updating of data sets. This report will be submitted also to peer-review after extensive internal review. Comments and suggestions are welcome.

Abstract

The first stage of the Integrated Precipitation and Hydrology Experiment (IPHEX) includes the development of quality-controlled data sets of different hydrometeorological and landscape attributes at high spatial and temporal resolutions (respectively 1km×1km and 1 hour). These data sets will facilitate the intercomparison of hydrological models and provide support to the ground validation campaign of GPM over the Southern Appalachian region. In the present report we focus on the spatial downscaling of Stage IV precipitation data (Baldwin and Mitchell, 1996; Lin and Mitchell, 2005; see online at http://www.emc.ncep.noaa.gov/mmb/ylin /pcpanl/stage4) from 4km to 1km resolution for the period 2007-2011. First, we describe the methodologies utilized to develop the various QPE products and in particular the use of modified fractal downscaling methodologies, which conserve the spatial structure of the coarse resolution while enhancing sub-grid scale variability. Three different (hourly, $1km^2$) precipitation datasets were produced: 1) Stage IV bilinear interpolated fields; 2) Stage IV fractal downscaled fields using β_{Ens} (with 50 ensemble realizations for each hour); and 3) Stage IV fractal downscaled fields using a transient β (with 50 ensemble realizations for each hour). The 50 realizations provided for each hour in the fractal downscaled cases should be particularly useful to ensemble hydrologic applications and analysis of uncertainty propagation. The performance of the downscaled QPE (Quantitative Precipitation Estimation) products is subsequently evaluated for selected headwater basins in the Southern Appalachians for individual events and for 5 year continuous simulations in three watersheds, which are intended to highlight that, in long-term hydrological modeling and prediction and the precipitation forcing is *de facto* not accurate, the uncertainty varies in time, and this is further modulated by storage, evapotranspiration and subsurface flow in the hydrological model, a highly nonlinear system. The results show

improved performance of an uncalibrated hydrological model using the downscaled Stage IV product using modified fractal interpolation methods as compared to bilinear interpolation. Finally, a survey of basic skill metrics indicates that current precipitation estimates are significantly poor in the inner mountain region of the Southern Appalachians where NEXRAD (Next Generation Radar Data) data used to inform the Stage IV product is compromised, which is expected in regions of complex terrain.

1. Introduction

The Integrated Precipitation and Hydrology Experiment (IPHEX) includes two major activities: the evaluation of QPE products for hydrologic forecasting and water resource applications in Southeast US (IPHEX-H4SE) and the first ground validation field campaign after the launch of NASA's Global Precipitation Measurement (GPM) satellite (IPHEX-GVFC). The focus of the first phase is on the generation of quality-controlled data sets over four major river basins - the Upper Tennessee, Catawba-Santee, Yadkin-Pee Dee and Savannah River (Figure 1) - all sharing the same grid with high spatial and temporal resolution (1km×1km and hourly time step) for the 2007-2011 period. These data sets include hydrometeorological and land-surface attributes extending over a wide range of scales.

All the datasets were firstly extracted from the original data sources: soil hydraulic parameters are derived from the State Soil Geographic (STATSGO) database, landscape attributes datasets are derived from Environmental Moderate Resolution Imaging Spectroradiometer (MODIS) products, atmospheric forcing data are derived from the North American Regional Reanalysis (NARR), and precipitation is derived from NCEP/EMC 4KM Gridded Data (GRIB) Stage IV dataset (Baldwin and Mitchell, 1996; Lin and Mitchell, 2005; see online at http://www.emc.ncep.noaa.gov/mmb/ylin/pcpanl/stage4). They are re-projected to UTM17N (WGS84) and interpolated to the domain grid system at 1km×1km resolution. Finally corrections and adjustments are applied to improve these datasets, resulting in a 1km resolution five-year best estimates "historical" data set which will be provided to all H4SE participants at the website of IPHEX(http://iphex.pratt.duke.edu/) allowing for a robust inter-comparison and evaluation of hydrological models performance on a selected number of case studies. It will also serve as basis for real-time forecasting activities supporting the Intense Observing Period (April-July

2014), evaluation of GPM precipitation algorithms as well as for evaluation of satellite-based rainfall products in hydrologic applications including water resources management and forecasting of natural hazards such as flash floods, riverine floods and landslides. In the present report, the focus is on the high resolution hourly precipitation estimates over the Southern Appalachian region, in particular the Pigeon River Basic. After re-projection of Stage IV precipitation estimates at 4km resolution to UTM17N, three downscaled products at 1km resolution were generated (summarized in Table 1): the first using simple bilinear interpolation and two others using stochastic modified fractal interpolation algorithms.

The development of stochastic downscaling strategies from coarser resolution data has been a very active research topic in the past few decades. Stochastic downscaling schemes aim to reproduce the sub-grid scale rainfall variability over a desired range of spatial and/or temporal wavelengths by adding realistic (statistically) high-frequency heterogeneity, hence increasing the information content of coarser datasets to meet the resolution requirements for hydrometeorological and hydrological applications amply discussed in the literature (e.g. Bindlish and Barros 2000; Deidda, 2000; Harris et al., 2001; Ferraris et al., 2003; Rebora et al., 2006, among others). In the last 30 years, a broad number of investigations have reported spatio-temporal multifractal behavior of rainfall fields (and other geophysical quantities) across wide ranges of scales, on both observed and numerically simulated fields (see e.g. Nogueira et al, 2013 and references therein). This (statistical) scaling behavior implies that statistical properties across different scales are related by power laws, a property of obvious importance for numerical modeling sub-grid parameterization and downscaling applications that should reproduce the scaling behavior if they are to generate realistic fields.

Several downscaling schemes based on modified fractal interpolation methods have been developed to preserve the scaling behavior and generate statistically coherent sub-grid scale variability. Despite the methodology differences among these schemes, all of the various downscaling algorithms are able to reproduce the main statistical properties of rainfall including anomalous scaling and add statistically relevant information in the sub-grid scales, such as significant enhancements in the spatial variability (see e.g. Rebora et al., 2006, Tao and Barros, 2010 and Garborit et al., 2012 for reviews). The downscaling procedures used here are based on previous work of Bindlish and Barros (1996) and subsequent work by Rebora et al. (2006), where a simple modified fractal interpolation is used for spatial disaggregation of a geophysical field in the Fourier spectral domain. Two QPE products obtained by two alternative implementations of this methodology are made available: one using the scaling parameters estimated from ensemble statistics (StageIV_FF) and another obtained by introducing a modification into the first scheme to account for the transient dynamical dependence of the scaling parameters, estimating them for each realization from the respective coarse resolution field power spectrum (StageIV_TF).

The Pigeon River Basin, PRB (shown in Figure 1) was chosen as the test-bed for the hydrological simulation experiments for verification of the 1km resolution datasets. Both fractal interpolated rainfall fields (StageIV_FF and StageIV_TF) are compared against a control bilinear interpolation of Stage IV to 1 km resolution (StageIV_Bi). The experiments are conducted for three sub basins that are equipped with USGS stream gauges, but not limited by dam operations in the PRB, including the Cataloochee Creek Basin (CCB), the West Fork Pigeon River Basin area (WFPRB) and the East Fork Pigeon River Basin (EFPRB). These are relatively small (<200 km^2) headwater catchments which provide a good reference to evaluate the precipitation products without introducing the average effects of the simulations at large scales. They extend for a period of roughly 5 years (2007 – 2011) during which all datasets are available for the study region.

The organization of this report is as follows: Section 2 describes the methodology for fractal interpolation of precipitation fields from Stage IV 4km resolution to 1km. Section 3 presents statistical error analysis on the downscaled products and Section 4 presents hydrological application experiments over the Pigeon River basin using the 3D-LSHM driven by the different high-resolution precipitation datasets both the raw and the adjusted landscape attributes datasets, to evaluate their performance in hydrological applications. The summary and final remarks are provided in Section 5.

2. Modified fractal interpolation downscaling

In the present investigation we focus on downscaling methodologies in the Fourier spectral framework, due to their theoretical and implementation simplicity, their ability to preserve the spatial and temporal structure in the coarse resolution information while enhancing variability in the smaller unresolved scales, their continuity in the spectral domain and their quickness of computation. These models have been applied successfully in the past to rainfall and other geophysical fields (e.g. Bindlish and Barros, 1996, 2000; Rebora et al., 2006; Brussolo et al., 2009; Tao and Barros, 2010). Spatial scaling invariance manifests itself as log-log linearity of the power spectrum in space:

$$E(k) \sim k^{-\beta-1} \qquad (1)$$

where β is the spectral exponent and $E(k)$ is the isotropic power spectrum, obtained by angularly averaging the 2-dimensional spatial Fourier power spectrum, $E(k_x, k_y)$, k_x and k_y are respectively the wavenumber components in the x and y directions and $k = \sqrt{{k_x}^2 + {k_y}^2}$. Consequently, β can be estimated using least square regression in log-log plots. The addition of -1 in the exponent is required due radial averaging is phase space (Turcotte, 1992).

By preserving the known, coarse resolution, portion of the power spectrum and extrapolating it to sub-grid scale wavenumbers using the correct spectral slope and amplitude, one can obtain a higher-resolution downscaled version of the field that preserves the spatial structure and correct scale invariant behavior, with coherent variability at the fine scales (Figure 2). Based on previous works of Bindlish and Barros (1996), this can obtained by generating a modified fractal Brownian surface (fBs) with the desired fine resolution, number of grid points and correct spectral exponent, then normalize it and use it as an interpolation surface. The preservation of the exact coarse resolution information can be obtained by normalizing the fBs by a coarse resolution version of itself at the same resolution as the original coarse data (see Rebora et al., 2006 for details). This method requires a priori knowledge of the "correct" spectral slope β which is not a trivial problem. The simplest approach is to assume the value $\beta_{ens} \approx 1.9$ estimated from the ensemble statistics of hourly rainfall fields over 3 years period at 1 km resolution and over the Southern Appalachians region (Figure 3), using cluster analysis to take into account for the effect of large fractions of zeros on the rainfall scaling (Nogueira et al., in production). This fixed (ensemble) spectral slope value assumption corresponds to downscaled product StageIV_FF. Another downscaling product, StageIV_TF, is created taking into consideration the fact that there is a widespread range of values of the scaling parameters for rainfall fields in the literature (see Tuck, 2010 for a review) and highly dynamic variation of fractal parameters has been reported in previous works that found linkages between the scaling and mean atmospheric and topographic properties (Over and Gupta, 1994; Perica and Foufoula-

Georgiou, 1996; Barros et al., 2004, Nykanen, 2008; Nogueira et al., 2013). Consequently, if statistical scaling based methods are to be used for downscaling particular realizations of rainfall fields they have to be able to reproduce this variability and dependences. However, the relationships between scaling parameters and system state variables display complex nonlinear character (Nogueira et al., 2013), and hence well-defined quantitative expressions haven't been established. Here we use a simple approximation using least-square regression on log-log power spectra computed from Stage IV resolution data to estimate β for each single realization, i.e. each hourly rainfall field, to be downscaled. The fact that Stage IV data corresponds to a large high-resolution grid (179×153 grid points at 4 km resolution) allows for robustness in these spectral slope estimates. Each β estimate is used to generate the fBs to downscale the respective rainfall realization.

A further source of complexity comes from the fact that some geophysical fields, such as rainfall and clouds, are heavily physically thresholded and have large fractions of zero values. Additionally, any measurement no matter how precise has an associated measurement threshold contributing to increase the fraction of zeros in the measure field, and distinguishing between measurement and physical zeros becomes virtually impossible for most applications and datasets. The fractal interpolation methodology does not create any new zeros in the downscaled field, which is not realistic (see e.g. Lovejoy et al., 2008; Verrier et al., 2010). A simple way to account for this factor and generate new zeros is to add a thresholding operation to the downscaled field, where all values below a certain threshold are set to zero. This method has been used in the past with good performance in replicating the number of zeros in the high-resolution fields (Perica and Foufoula-Georgiou, 1996; Rebora et al., 2006; Lovejoy et al., 2008, Verrier et al., 2010; Garborit et al., 2012). Here we chose the threshold value of 0.1 mm/hour which showed good performance in reproducing the number of zero pixels in high resolution fields on preliminary tests.

3. Datasets and error analysis

As stated in Section 1, if a model is to generate realistic rainfall fields it should be reproduce the observed scale invariant behavior. Based on this concept a possible verification of the downscaled datasets is to investigate the ability of interpolated fields to reproduce the expected scaling according to the observations, taken the assumption that the mean scaling behavior found in StageIV data 4 km resolution extends down to the 1km resolution, which is supported by previous studies (e.g. Tao and Barros, 2010; Verrier et al., 2010; Nogueira et al., 2013 among others). Three different products with hourly temporal resolution and 1km^2 spatial resolution are made available for this first phase of H4SE (summarized in Table 1):

1) Stage IV bilinear interpolated fields to 1km resolution (StageIV_Bi);
2) Stage IV fractal downscaled fields using β_{ens}, with 50 realizations for each hour (StageIV_FF);
3) Stage IV fractal downscaled fields using β transient, with 50 realizations for each hour (StageIV_TF);

The 50 realizations provided for each hour in the cases of StageIV_FF and StageIV_TF should be particularly useful to ensemble hydrologic applications and analysis of uncertainty propagation. The intercomparison between the spectral exponents computed from downscaled products against the 4km resolution Stage IV, β_{STIV} is shown in Fig. 4a. The smoothing introduced by the bilinear interpolation method causes a large drop in the variability at the smallest-scale and hence an abrupt increase in β corresponding to a large overestimation of the expected spectral exponent, with several occurrences of unphysical $\beta > 3$ values. The use of $\beta_{ens} = 1.9$ to downscale all times causes the downscaled spectra to display scaling exponents around this ensemble value which is unrealistic in single realizations where the observations show significantly lower (or higher) slopes. This can be quantified by computing the Mean Absolute Error between downscaled field and original Stage IV ($MAE = (\frac{1}{N})\sum|\beta_{Dws} - \beta_{STIV}|$), resulting in values of 0.25 for StageIV_TF, 0.38mr for StageIV_FF and 1.18 for StageIV_Bi. The fact that fractal methodologies, and particularly StageIV_TF, are better in reproducing the StageIV scaling behavior is expected and in agreement with the methodologies. These results are valid for cases with the linear regression coefficient for β estimation is $r^2 > 0.98$, hence where variability should correspond to a physical transient behavior of the scaling exponents and not associated with problems in the estimation of the spectral exponent. It becomes clear that the use of β_{ens} is not a good approach for all times and the transient nature of the scaling exponent should be taken into account and consequently StageIV_TF product is a better approximation to the real scaling behavior of the observed rainfall fields.

Finally the average probability density function (PDF) during the five year period over the raingauges in the PBR region (described in Table 2) are computed and compared against the PDF for each of the downscaling products, using nearest pixel approximation to obtain point values over the raingauge locations. All downscaling products show clear underestimation of the low intensity (< 5 mm/hr) precipitation frequency (Fig. 5), which is associated with problems in the weather radar used in StageIV to identify such values. Note that this is likely to cause problem for water cycle evaluation as light rainfall represents a substantial part of the water brought in the Appalachians. For intermediate intensities, all products show good reproduction of the raingauge observations, particularly considering the comparison is between point measurements and 1km resolution gridded data. This fact should also be responsible for the general PDF underestimation at the highest intensities for all gridded products. The smoother bilinear interpolation product causes the largest underestimation as expected. The smoothing introduced by the ensemble averaging operations in StageIV_FF and StageIV_TF products is also associated with frequency decrease in the highest intensities, as can be seen by comparing against a randomly chosen single realization results out of the 50 realizations available at each time step (light blue and pink lines). The results for StageIV_TF have slightly higher PDF values than StageIV_FF, which is explained by the fact that many cases display lower spectral exponents (Fig. 4), and hence less smoothing, than the considered $\beta_{ens} = 1.9$ in StageIV_FF.

4. Results

To illustrate the utility of the rainfall products in hydrologic studies for the IPHEx-H4SE, streamflow simulations were conducted in the Pigeon River Basin (shown in Figure 1) using a physically-based fully-distributed hydrological model (3D-LSHM) forced by randomly selected single realizations of the two fractal downscaling products (StageIV_FF and StageIV_TF) and bilinear interpolation of StageIV to 1km resolution (StageIV_Bi). The simulations were conducted continuously from January/2007 to December/2011 in three unimpaired headwater catchments in the Pigeon River Basin equipped with USGS stream gauges, including the Cataloochee Creek Basin (CCB, 128km^2), the West Fork Pigeon River Basin (WFPRB, 71km^2) and the East Fork Pigeon River Basin (EFPRB, 131km^2), are used to compare with streamflow observations and then to validate the accuracy of the rainfall products.

Two particular events were selected for detailed analysis. One is Tropical storm Fay in August of 2008 which caused extensive flash floods in the basins and has been investigated by previous study using the same hydrologic model at very high resolution (250m and 5min) (Tao and Barros, 2013b). The other is a winter storm causing debris flow events in the Pigeon River Basin of which the initiation mechanism has been investigated also at high resolution (Tao and Barros, 2013a).

In this study, the hydrological simulations were conducted at the IPHEx-H4SE conventional scale of 1km×1km spatial resolution and hourly temporal resolution. Spatial soil moisture for all times including storms selected are the same as used in Tao and Barros (2013b) but averaged to the 1km × 1km resolution and hourly resampled. Note, the 3D-LSHM is uncalibrated and without any manual tuning against the observations, because our goal here is to demonstrate the uncertainty in hydrological simulations induced by rainfall input datasets, and to document the long-term evolution of propagating uncertainty in rainfall by hydrological simulations. The adjusted landscape attributes including the broadband albedo and emissivity, LAI and CV after post processing (e.g. quality control and the Savitzky-Golay filtering), and the adjusted atmospheric forcing datasets including atmospheric temperature, atmospheric pressure, specific humidity, wind speed, downward longwave radiation and shortwave radiation corrected for elevation effects, topographic and cloudiness effects, are used as the forcing datasets to the 3D-LSHM. Detailed description about the adjustment for these datasets can be found in other two reports associated with IPHEx-H4SE (Report EPL-2013-IPHEX-H4SE-1 and Report EPL-2013-IPHEx-H4SE-2).

One-year spin-up simulations were conducted before the real simulation proper to reach internal consistency in the model. The streamflow simulations results in operational-like mode in the

WFPRB for the two selected storm events are shown as examples in Figure 6 and the Nash-Sutcliffe efficiency (NSE) are shown in Table 3. The closer the NSE is to unity, the better the performance. Overall the StageIV data demonstrate good performance, with StageIV_FF and StageIV_TF clearly outperforming the StageIV_Bi displaying higher NSE. The simulations using the StageIV_FF and StageIV_TF show very similar performance with NSE values close to each other. Note that the performance for fractal downscaling are similar to results reported by Tao and Barros (2013a) using a locally enhanced precipitation product by introducing the influence of the dense network (Pratt and Barros, 2010) which is not included in the Stage IV products used here. For the Tropical storm event shown in Figure 6a, the StageIV_FF and StageIV_TF show lower NSE, but with good peak values and falling limbs. For the winter storm shown in Figure 6b, the StageIV_FF and StageIV_TF display NSEs very close to unity with well captured times-to-peak and the peak values of the hydrographs. Figure 7 shows the cumulative basin-averaged rainfall depth (dash lines) and streamflow (solid lines) in the WFPRB for the two simulated events. As it can be seen from the figure, the total runoff volume of the simulated streamflow using StageIV_FF and StageIV_TF are very close to the observations for the two events, whereas the integrated volume of the simulated streamflow using the StageIV_Bi shows much less runoff compared to the observed streamflow. Indeed, the cumulative depth of StageIV_Bi is always less than StageIV_FF and StageIV_TF, which is attributed to smoothing by the bi-linear interpolation. The spatial distributions of the cumulative rainfall in the Pigeon River Basin for the two events are given in Figure 8. The StageIV_Bi rainfall fields are smoother than the StageIV_FF and StageIV_TF, losing some water mass at the boundaries of 4km pixels of original StageIV data. Both StageIV_FF and StageIV_TF enhance variability on scales $< 4km$, while conserving the mean value at the original StageIV 4km resolution, that is they are mass conserving. Note that even though StageIV is in fact a merged radar and raingauges product provided by RFCs (River Forecasts Centers), it contains little to no information over the Pigeon river basin which is not covered by the NEXRAD network in the Southern Appalachians, and where there is very limited operational raingauge information. Consequently, it is noteworthy that the StageIV_FF and StageIV_TF produce good simulation results. Generally, the radar-gauge merged products such as StageIV have better accuracy in the Piedmont and Coastal Plains regions than in the mountainous regions.

One continuous streamflow simulation without re-initialization was conducted using the uncalibrated hydrologic model described in Tao and Barros (2013a and 2013b) in the three headwater catchments of the Pigeon River Basin including the WFPRB (West Fork), EFPRB (East Fork) and CCB (Cataloochee) are shown in Figure 9 for the five year period from 2007 to 2011 using the data sets described in EPL-IPHEX-H4SE-1 and EPL-IPHEX-H4SE-2. This simulation serves as a baseline example of the propagation of uncertainty of the precipitation products through a hydrologic model without calibarion or reinitialization as would be expected in routine operational hydrology. Overall, the StageIV_FF and StageIV_TF again perform better than StageIV_Bi which generally underestimates streamflow. It should be stressed that, the WFPRB and the EFPRB are located at very high elevation on the eastern slopes of the Appalachians where the mountain blockage to the radar scan is not as severe as in the basins located in the inner region low elevation or valleys, such as the CCB (see Figure 1). Without low-level raingauge observations in the valleys, radar-based rainfall products cannot resolve the rainfall gradient along ridges to valleys, thus cannot provide accurate rainfall data in the inner region. Consequently, all simulations independently of rainfall datasets overestimate streamflow in the CCB as shown by the bottom panel in Figure 9. Finally, note the decrease in the 5-year hourly NSE score between the WFPRB, the EFPRB and the CCB basins independently of rainfall forcing. This reflects the significant differences in the governing hydrological processes from one basin to another due to local hydrogeology and landslide activity that has contributed for significantly thicker soil depths across the CCB and in the valley in the EFPRB.

To evaluate the impact of initial basin storage, a test simulation for the EFPRB including 15-years of spin-up period is described in EPL-IPHEX-H4SE-1. The spin-up consisted in re-running the 5-year simulation three times using the same 5–year forcing. Results show that the 5-year NSE (Nash-Sutcliffe efficiency) score for hourly streamflow simulations increases from 0.28 to 0.45, an improvement of 61% (see Figure 25 in EPL-IPHEX-H4SE-1). This implies that there are still unaccounted for forcing errors, especially in the rainfall as discussed above, but the NSE score reported in Table 2 overestimates the error fraction due to rainfall forcing alone. This example illustrates the highly nonlinear and complex interactions among hydrologic processes and basin geomorphic characteristics, which can have a strong impact on error attribution and error propagation.

5. Final remarks and Recommendations

In summary the modified fractal downscaling methodologies generate statistically robust 1km resolution fields without any additional data or calibration requirements. These fields conserve the structure in the StageIV observations at 4km resolution and enhance the small-scale variability and statistics, adding value to the original field a displaying more coherent structure than bilinear interpolation which smoothes out much of the small-scale variability. The hydrological simulations shown here, conducted without any calibration or adjustment of the hydrological model, show that for operational hydrology applications, in which case capturing the long-term variability of the water cycle is not of essence, and therefore model calibration is desirable, the StageIV_FF or StageIV_TF should be a robust QPE product for hydrological applications in IPHEx-H4SE. Based on the results of Section 3 error analysis and Section 4 using hydrological model simulations, we recommend the use of StageIV_TF. Users interested in further downscaling products at higher resolutions should contact the authors.

References

Baldwin, M.E., and K.E. Mitchell, 1998: Progress on the NCEP hourly multi-sensor U.S. precipitation analysis for operations and GCIP research. Preprints, 2nd Symposium on Integrated Observing Systems, 78th AMS Annual Meeting, 10-11.

Barros, A. P., Kim, G., Williams, E., and Nesbitt, S. W., 2004: Probing orographic controls in the Himalayas during the monsoon using satellite imagery. Nat. Hazards Earth Syst. Sci., 4, 29–51.

Bindlish, R., and Barros., A. P., 1996: Aggregation of digital terrain data using a modified fractal interpolation scheme. Comput. Geosci. (UK), 22, 907 – 917.

Bindlish, R., and Barros, A. P., 2000: Disaggregation of rainfall for one-way coupling of atmospheric and hydrological models in regions of complex terrain. Global and Planetary Change, 25, 111-132.

Brussolo, Elisa, Jost von Hardenberg, and Nicola Rebora, 2009: Stochastic versus Dynamical Downscaling of Ensemble Precipitation Forecasts. J. Hydrometeor, 10, 1051–1061

Deidda, R, 2000: Rainfall downscaling in a space-time multifractal framework. Water Resour. Res., 36, 1779–1794.

Ferraris L, Gabellani S, Rebora N, Provenzale A. 2003. A comparison of stochastic models for spatial rainfall downscaling. Water Resources Research 39, SWC 12-1.

Gaborit, É., Anctil, F., Fortin, V. and Pelletier, G., 2013: On the reliability of spatially disaggregated global ensemble rainfall forecasts. Hydrol. Process., 27, 45–56.

Harris, D., Foufoula-Georgiou, E., Droegemeier K. K., and Levit, J. J, 2001: Multiscale Properties of a High-Resolution Precipitation Forecast, J. Hydrometeor., 2, 406-418.

Kim, D., Nelson, B., Seo, D.J., 2009. Characteristics of Reprocessed Hydrometeorological Automated Data System (HADS) Hourly Precipitation Data. Weather and Forecasting, 24(5): 1287-1296.

Lin, Y. and K. E. Mitchell, 2005: The NCEP Stage II/IV hourly precipitation analyses: development and applications. Preprints, 19th Conf. on Hydrology, American Meteorological Society, San Diego, CA, 9-13 January 2005, Paper 1.2.

Lovejoy, S., Schertzer, D., and Allaire, V., 2008: The remarkable wide range spatial scaling of TRMM precipitation. Atmos. Res., 90, 10-32.

Nelson, B.R., Seo, D.J., Kim, D., 2010. Multisensor Precipitation Reanalysis. Journal of Hydrometeorology, 11(3), 666-682.

Nogueira, M., Barros, A. P., and Miranda, P. M. A., 2013: Multifractal properties of embedded convective structures in orographic precipitation: toward subgrid-scale predictability. Nonlin. Processes Geophys., 20, 605-620.

Nogueira, M., Barros, A. P., and Miranda, P.M.A,: Dynamical spatial downscaling of surface precipitation using multifractal and cluster methods

Nykanen, D. K., 2008: Linkages between Orographic Forcing and the Scaling Properties of Convective Rainfall in Mountainous Regions. J. Hydrometeor, 9, 327–347.

Over, T. M., and Gupta, V. K., 1994: Statistical analysis of mesoscale rainfall: Dependence of a random cascade generator on large-scale forcing. J. Appl. Meteor., 33, 1526–1542.

Perica, S., and Foufoula-Georgiou, E., 1996: Linkage of scaling and thermodynamic parameters of rainfall: Results from midlatitude mesoscale convective systems. J. Geophys. Res., 101, D3. 7431–7448.

Prat, O. P., and Barros, A. P., 2010. Assessing satellite-based precipitation estimates in the Southern Appalachian Mountains using raingauges and TRMM PR. Advances in Geosciences. 25, 143-153.

Rebora, N., Ferraris, L., von Hardenber, J., and Provenzale, A., 2006: RainFARM: Rainfall Downscaling by a Filtered Autoregressive Model. J. Hydrometeor., 7, 724-738.

Seo, D.J., 1998. Real-time estimation of rainfall fields using rain gage data under fractional coverage conditions. J. Hydrol., 208(1-2), 25-36.

Seo, D.J., and Breidenbach, J.P., 2002. Real-time correction of spatially nonuniform bias in radar rainfall data using rain gauge measurements. J. Hydrometeorol., 3(2), 93-111.

Tao, Kon, and Barros, A.P., 2010: Using Fractal Downscaling of Satellite Precipitation Products for Hydrometeorological Applications. J. Atmos. Oceanic Technol., 27, 409–427

Tao, J., and Barros, A.P., 2013a. Coupled prediction of flood response and debris flow initiation during warm and cold season events in the Southern Appalachians, USA. Hydrol. Earth Syst. Sci. Discuss., 10(7): 8365-8419.

Tao, J., and Barros, A.P., 2013b: Prospects for Flash Flood Forecasting in Mountainous Regions–An Investigation of Tropical Storm Fay in the Southern Appalachians. J. Hydrol.

Tao, J. and Barros, A.P., 2013: The Integrated Precipitation and Hydrology Experiment. Part I: Quality High-Resolution Landscape Attributes Datasets. Report EPL-2013-IPHEX-H4SE-1, EPL/Duke University (Pub.), V.1., 60 pp. DoI: Duke University Libraries (request pending)

Tao, J. and Barros, A.P., 2013: The Integrated Precipitation and Hydrology Experiment. Part II: Atmospheric Forcing and Topographic Corrections. Report EPL-2013-IPHEX-H4SE-2, EPL/Duke University (Pub.), V.1., 80pp. DoI: Duke University Libraries (request pending)

Turcotte, D. L., 1992: Fractals and chaos in geology and geophysics. Cambridge University Press, New York, 221 p.

Verrier S., De Montera L., Barthès L., and Mallet C., 2010: Multifractal analysis of African monsoon rain fields, taking into account the zero rain-rate problem. Journal of Hydrology 389, 111-120.

List of Tables

Table 1 - Details of the different data sets.

Table 2 – Location, elevations and the data available period of rain gauges referenced in this study

Table 3 – Summary of NSE for hydrological simulations.

List of Figures

Figure 1 - The four drainage basins of interest in this project (shown on the right), namely Upper Tennessee River Basin(UTRB), Savannah River Basin(SVRB), Santee River Basin(SRB) and Yadkin-Pee Dee River Basin(YPDRB). The Pigeon River Basin (shown on the left), is the domain for the conducted hydrological verification at three sub basins that are not limited by dam operation in the Pigeon River Basin, including the Cataloochee Creek Basin (CCB), the West Fork Pigeon River Basin (WFPRB) and the East Fork Pigeon River Basin (EFPRB).

Figure 2 - Spectra interpolation schematic in the spectral domain: given the coarse resolution field (blue line), we extrapolate to sub-grid scale resolution using the correct spectral slope and amplitude (red line) to retrieve an approximation of the original high-resolution field (black line).

Figure 3 - Ensemble Fourier power spectrum computed from high-resolution rainfall fields only inside rain clusters (rainy regions) over the Southern Appalachians regions during a 3 year period (June-2008 to June-2011). The red-dashed line represents the least-square fit slope, corresponding to $\boldsymbol{\beta_{ens} = 1.9}$.

Figure 4 – Intercomparison of spectral exponent between downscaling products and original Stage IV data at 4km resolution, a) for all hourly rainfall fields during the 5 year period and b) only fields where the estimation of β in the coarse resolution data (StageIV) corresponds to a least-square regression with r^2>0.99.

Figure 5 – Intercomparison of probability density function (PDF) over the PRB raingauges (described in table 2) during the five year period. For 1km downscaled products nearest pixel approximation is used to obtain point values over the raingauge locations.

Figure 6 - Examples of streamflow simulations in the WFPRB for (a) a summer event (Tropical Storm Fay) in 2008 which caused flash floods in the basin and (b) a winter storm in 2009 which caused landslides in the region.

Figure 7 – Cumulative basin-averaged depth of rainfall (dash lines) and streamflow (solid lines) in the WFPRB for (a) the summer event in 2008 and (b) the winter storm in 2009.

Figure 8 - Spatial distribution of the cumulative rainfall in the Pigeon River Basin for (a) the summer event in 2008 and (b) the winter storm in 2009. The watershed boundaries of WFPRB, EFPRB and the CCB are illustrated by dark polygons.

Figure 9 - Continuous streamflow simulations in the WFPRB, EFPRB and CCB from the top to the bottom, for the Q2 data available period which is from Jul. 2008 to Oct. 2011

Name	Dataset description	Resolution	Period of availability	Domain of availability
StageIV	Original Stage IV dataset	4 km	Jan/2007 – Dec/2011	Full Southern Appalachians
StageIVBi	Stage IV downscaled to 1km using bilinear interpolation	1 km	Jan/2007 – Dec/2011	Full Southern Appalachians
StageIV_FF	Stage IV downscaled to 1km using fractal interpolation with ensemble β value.	1 km	Jan/2007 – Dec/2011	Full Southern Appalachians
StageIV_TF	Stage IV downscaled to 1km using fractal interpolation with transient β value.	1 km	Jan/2007 – Dec/2011	Full Southern Appalachians

Table 1 - Details of the different data sets.

NO.	Site		Lat.	Lon.	Elev.(m)	Collect Period
	Site ID.	Type				
1	RG001	GSMRGN (PMM)	35.39830	-82.91300	**1156**	2008 - 2011
2	RG002		35.41750	-82.97140	**1731**	
3	RG003		35.38460	-82.91610	**1609**	
4	RG004		35.36830	-82.99020	**1922**	
5	RG005		35.40890	-82.96460	**1520**	
6	RG008		35.38210	-82.97360	**1737**	
7	RG010		35.45640	-82.94680	**1478**	
8	RG100		35.58610	-83.07250	**1495**	Jun. 2008 - 2011
9	RG101		35.57500	-83.08820	**1520**	
10	RG102		35.56370	-83.10360	**1635**	Jul. 2008 - 2011
11	RG103		35.55340	-83.11790	**1688**	
12	RG104		35.55490	-83.08800	**1584**	
13	RG105		35.63900	-83.04050	**1345**	
14	RG106		35.43210	-83.02910	**1210**	Aug. 2008 - 2011
15	RG107		35.56810	-82.90750	**1359**	
16	RG108		35.55470	-82.98990	**1277**	
17	RG109		35.49560	-83.04040	**1500**	
18	RG110		35.54810	-83.14820	**1563**	
19	RG111		35.72970	-82.94780	**1394**	Sep. 2008 - 2011
20	RG112		35.75160	-82.96430	**1184**	
21	RG300		35.72653	-83.21692	**1558**	Jun. 2009 - 2011

22	RG301		35.70552	-83.25595	**2003**	
23	RG302		35.72135	-83.24675	**1860**	
24	RG303		35.76295	-83.16222	**1490**	
25	RG304		35.67010	-83.18287	**1820**	
26	RG305		35.69150	-83.13190	**1630**	
27	RG306		35.74597	-83.17148	**1536**	
28	RG307		35.65163	-83.19952	**1624**	
29	RG308		35.73027	-83.18237	**1471**	
30	RG309		35.68297	-83.15003	**1604**	
31	RG310		35.70273	-83.12263	**1756**	
32	RG311		35.76507	-83.14042	**1036**	
33	WAYN	ECONET	35.48752	-82.96768	840	2008 - 2011
34	CEPN7	HADS	35.46170	-82.87030	818	2008 - 2011
35	CTNN7		35.54830	-82.82890	863	
36	DARN7		35.35060	-82.77860	**1002**	2008 - 2011
37	LLDN7		35.42250	-82.92220	896	2008 - 2011
38	WAVN7		35.42640	-83.01030	943	
39	WLTN7		35.70330	-83.04140	735	

Table 2 – Location, elevations and the data available period of rain gauges referenced in this study

Simulation period	Basins	Precipitation Name	NSE
Aug. 25 – 28, 2008	WFPRB	StageIV_Bi	0.65
		StageIV_FF	0.78
		StageIV_TF	0.77
Jan. 5 – 10, 2009	WFPRB	StageIV_Bi	0.78
		StageIV_FF	0.89
		StageIV_TF	0.89
Jan/2007 – Dec/2011	WFPRB	StageIV_Bi	0.46
		StageIV_FF	0.51
		StageIV_TF	0.51
	EFPRB	StageIV_Bi	0.34
		StageIV_FF	0.36
		StageIV_TF	0.35
	CCB	StageIV_Bi	0.19
		StageIV_FF	0.22
		StageIV_TF	0.23

Table 3 – Summary of NSE for hydrological simulations.

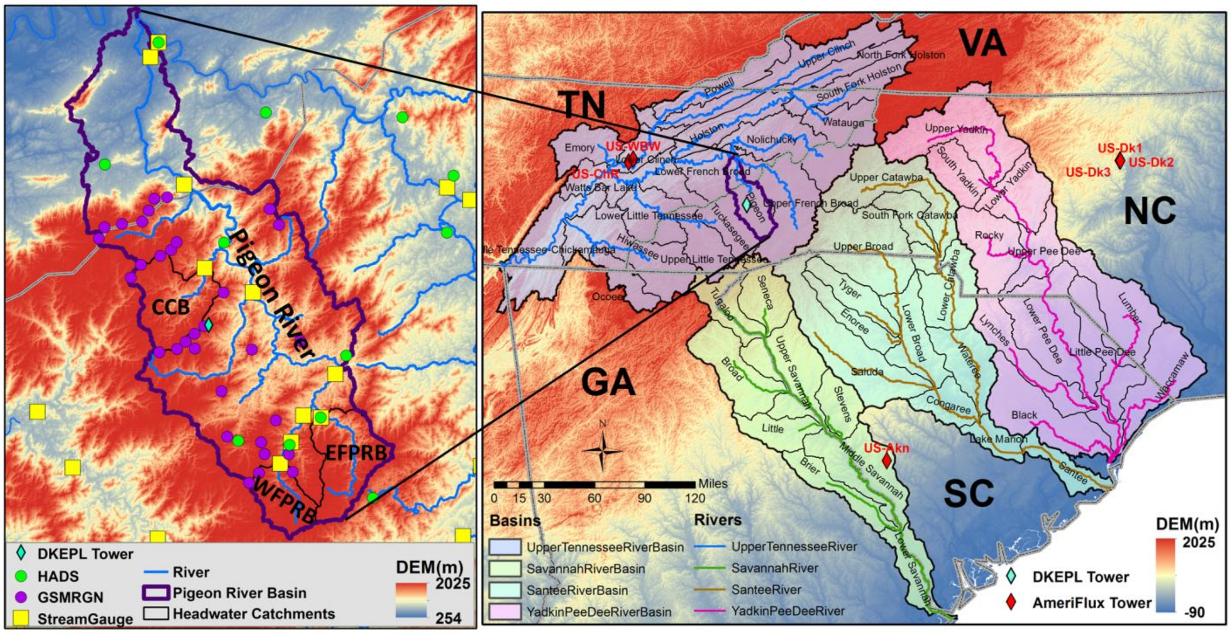

Figure 1 - The four drainage basins of interest in this project (shown on the right), namely Upper Tennessee River Basin(UTRB), Savannah River Basin(SVRB), Santee River Basin(SRB) and Yadkin-Pee Dee River Basin(YPDRB). The Pigeon River Basin (shown on the left), is the domain for the conducted hydrological verification at three sub basins that are not limited by dam operation in the Pigeon River Basin, including the Cataloochee Creek Basin (CCB), the West Fork Pigeon River Basin (WFPRB) and the East Fork Pigeon River Basin (EFPRB).

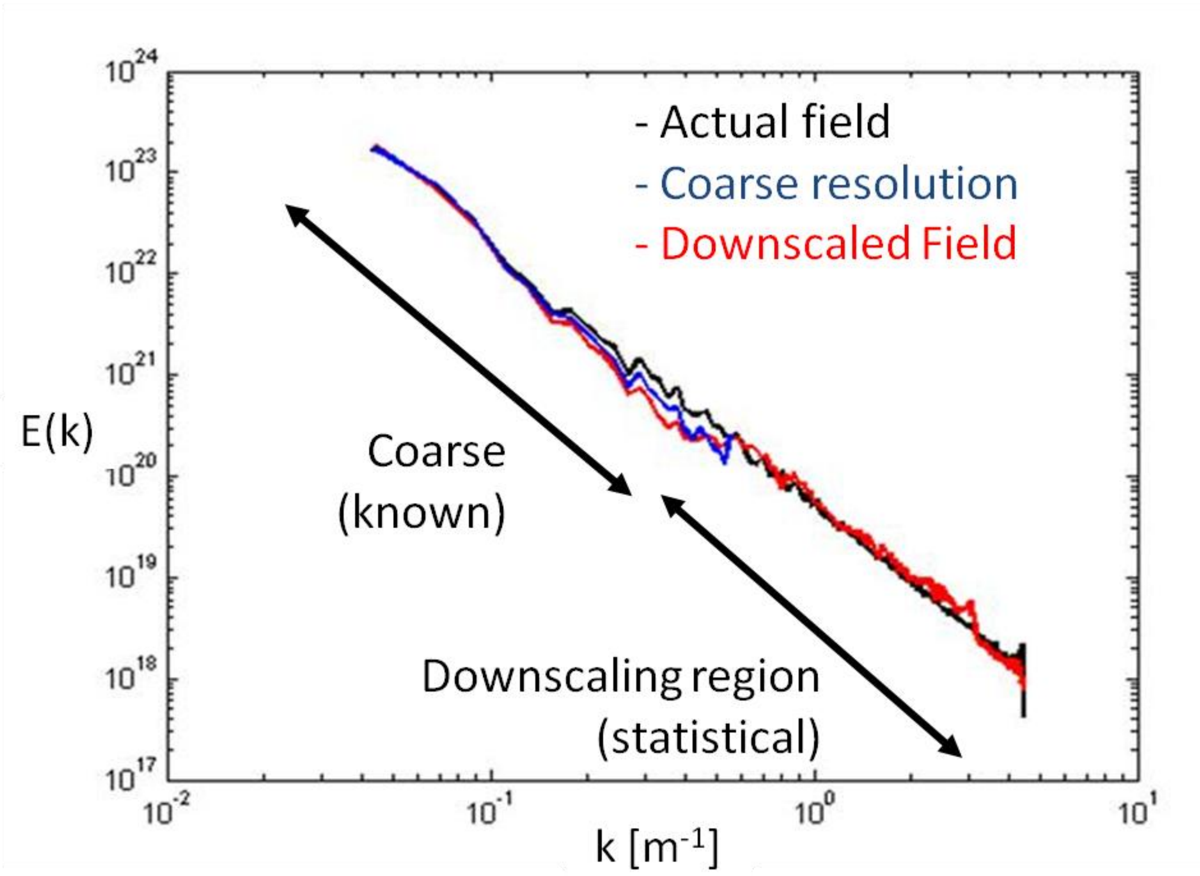

Figure 2 - Spectra interpolation schematic in the spectral domain: given the coarse resolution field (blue line), we extrapolate to sub-grid scale resolution using the correct spectral slope and amplitude (red line) to retrieve an approximation of the original high-resolution field (black line).

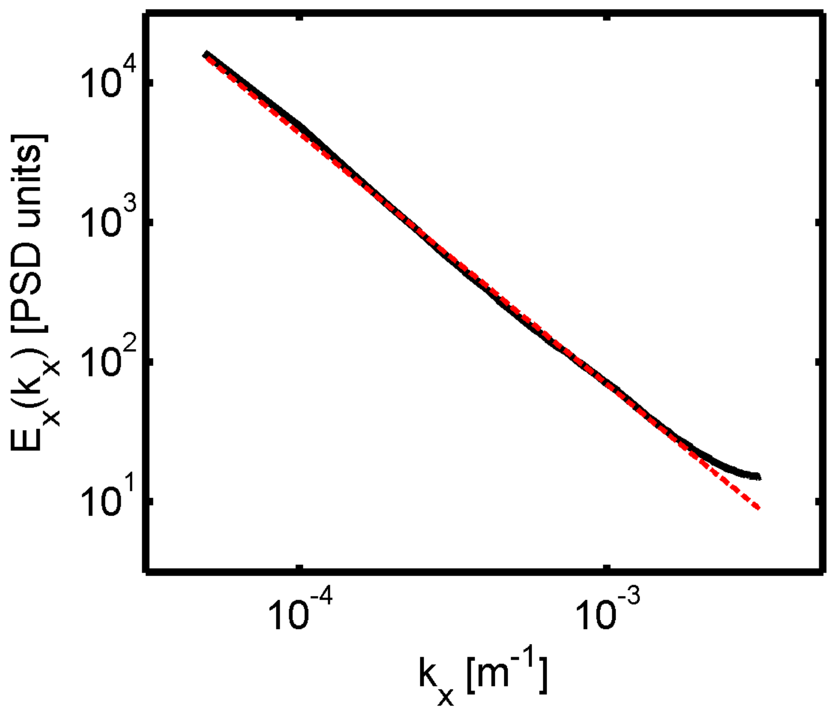

Figure 3 - Ensemble Fourier power spectrum computed from high-resolution rainfall fields only inside rain clusters (rainy regions) over the Southern Appalachians regions during a 3 year period (June-2008 to June-2011). The red-dashed line represents the least-square fit slope, corresponding to $\boldsymbol{\beta_{ens} = 1.9}$.

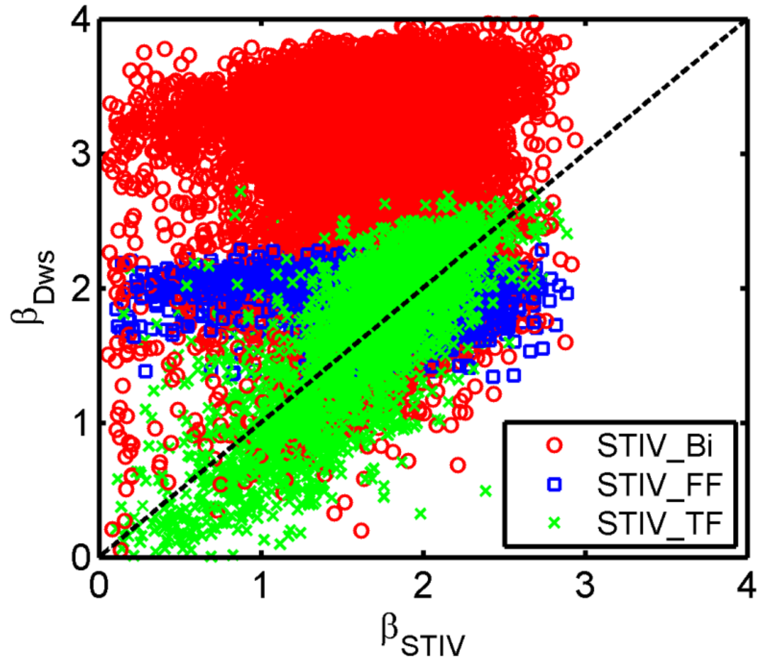

Figure 5 – Intercomparison of spectral exponent between downscaling products and original Stage IV data at 4km resolution, for fields where the estimation of β in the coarse resolution data (StageIV) corresponds to a least-square regression with r^2>0.98.

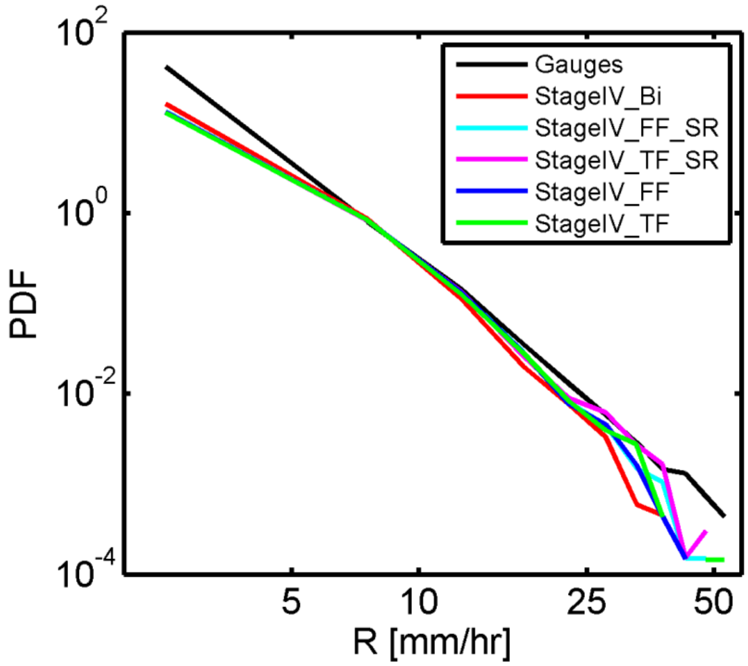

Figure 5 – Intercomparison of probability density function (PDF) over the PRB raingauges (described in table 2) point locations during the five year period. Black line is computed from local raingauge data and the other lines corresponded to 1km resolution downscaled products. StageIV_FF_SR (light blue) and StageIV_TF_SR (pink) represent the statistiscs for a randomly chosen single realization (out of the 50 available) at each time instant. For 1km downscaled products nearest pixel approximation is used to obtain point values over the raingauge locations.

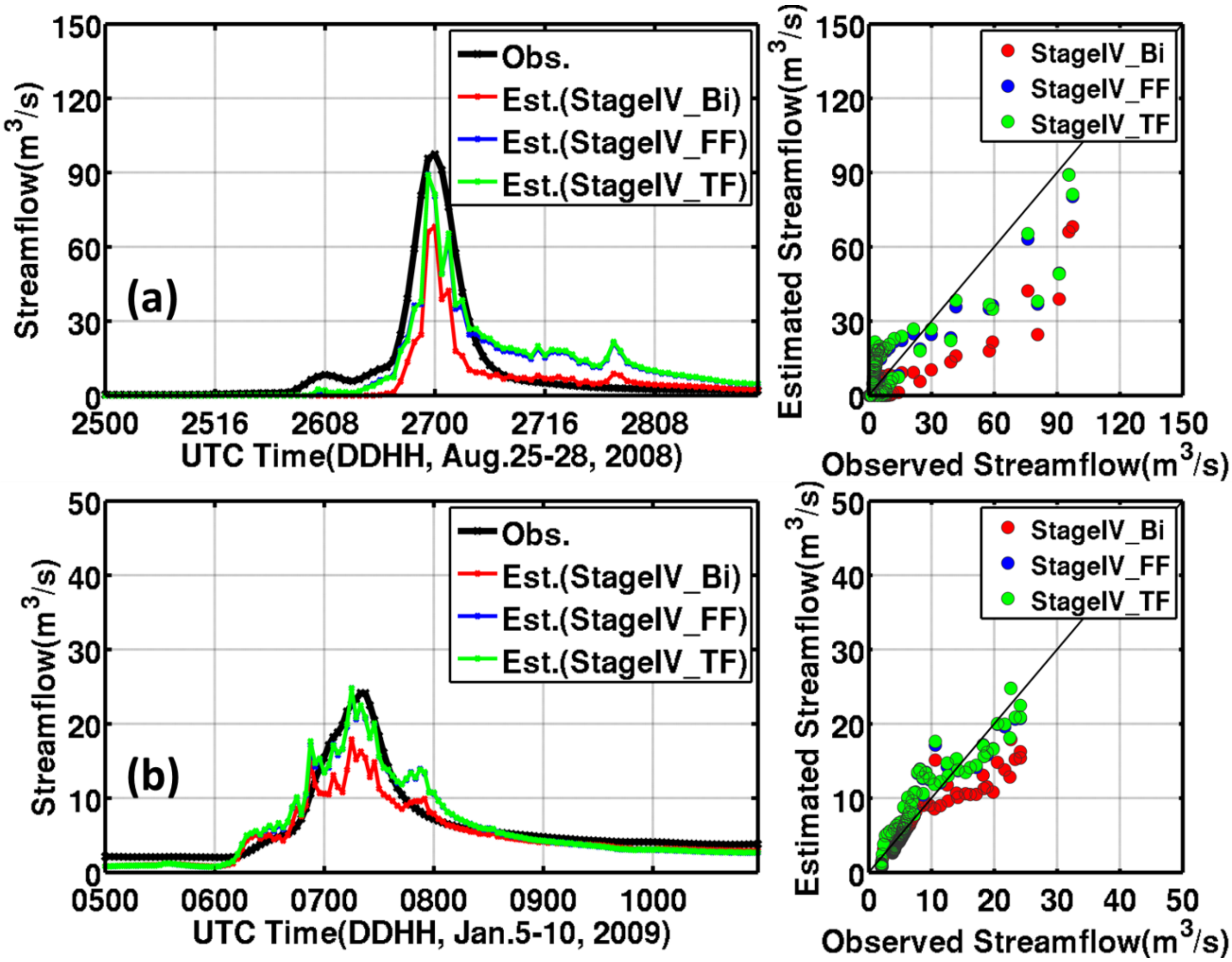

Figure 6 - Examples of streamflow simulations in the WFPRB for (a) a summer event (Tropical Storm Fay) in 2008 which caused flash floods in the basin and (b) a winter storm in 2009 which caused landslides in the region.

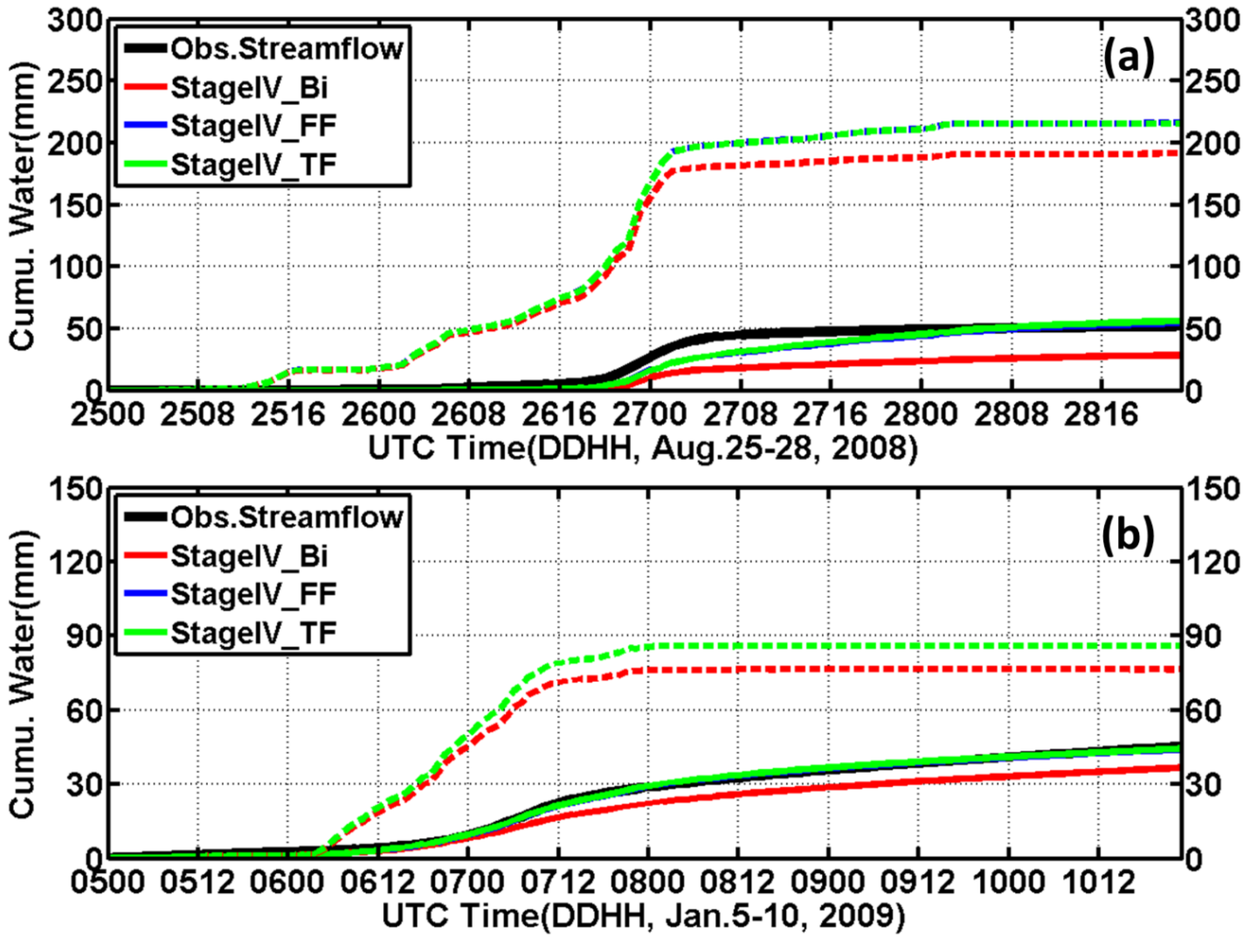

Figure 7 – Cumulative basin-averaged depth of rainfall (dash lines) and streamflow (solid lines) in the WFPRB for (a) the summer event in 2008 and (b) the winter storm in 2009. The rainfall plots from StageIV_FF and StageIV_TF are overlapped due to mass conversation.

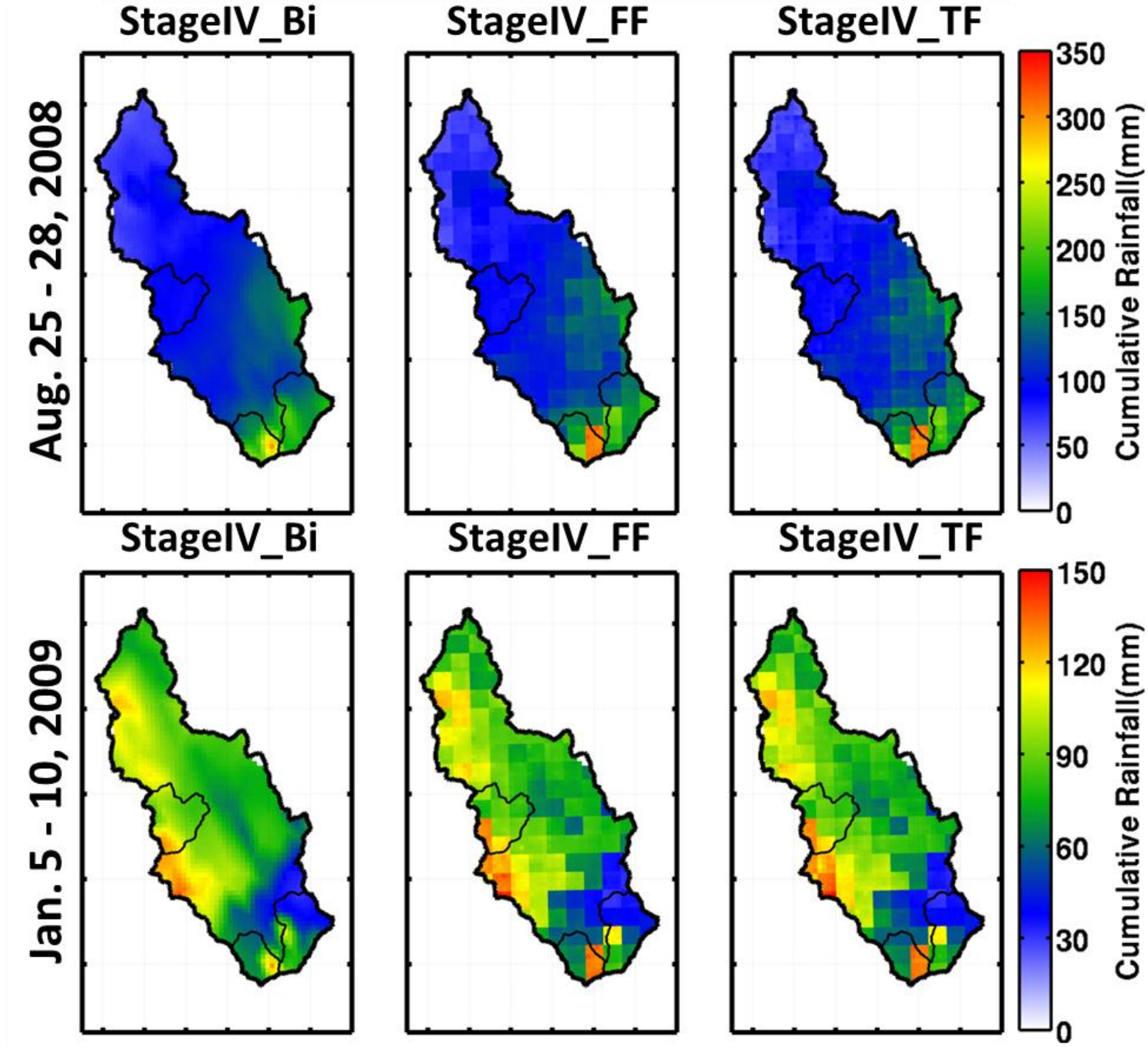

Figure 8 - Spatial distribution of the cumulative rainfall in the Pigeon River Basin for (a) the summer event in 2008 and (b) the winter storm in 2009. The watershed boundaries of WFPRB, EFPRB and the CCB are illustrated by dark polygons.

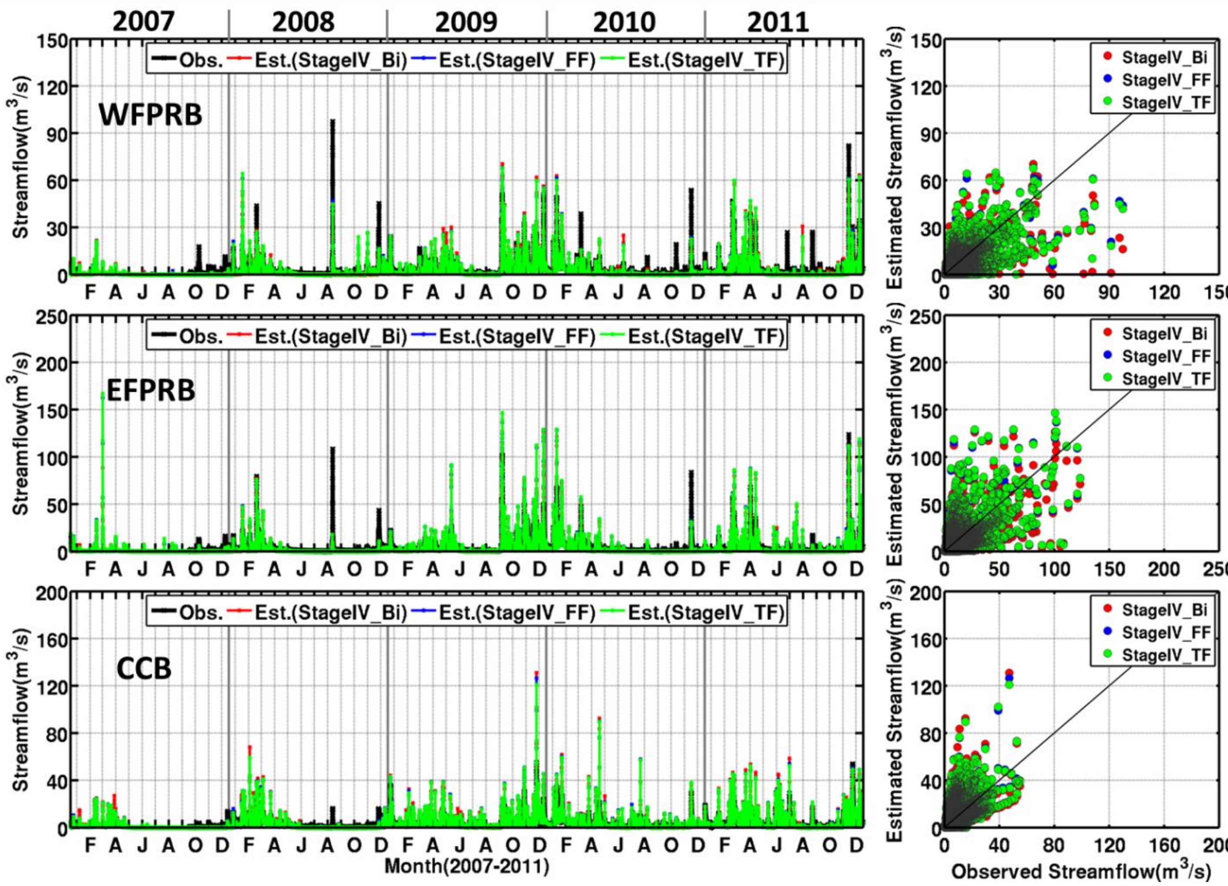

Figure 9 – Continuous 5-year streamflow simulations with the uncalibrated Duke-3DLSHM hydrologic model (1 km^2, 1 hr resolution in this implementation) forced by the StageIV_Bi and 50-realization ensemble means of the fractal downscaled StageIV products (StageIV_FF and StageIV_TF). The 5-year simulation was conducted without re-initialization or data assimilation; therefore, for individual events monitored by the NSE metric, it represents a worst case scenario in terms of initial conditions, specifically soil moisture. Note the decrease in NSE from top to bottom panels (Table 1), respectively for the WFPRB, EFPRB and the CCB. This reflects two critical factors in watershed hydrology: 1) the fidelity of the original StageIV data decreases strongly in the inner mountain region (e.g. CCB) and generally everywhere in the NEXRAD shadow regions; and 2) the rainfall errors are amplified in the EFPRB and CCB due to governing role of subsurface control on rainfall-runoff response (e.g. Tao and Barros, 2013).